JOURNAL OF APPLIED ELECTROCHEMISTRY 14 (1984) 425–436

Some theoretical considerations on the design of a practical anode in an electrochemical reactor

OSCAR LANZI, ROBERT F. SAVINELL

Department of Chemical Engineering, The University of Akron, Akron, Ohio 44325, USA

RICHARD E. HORN

Electrochem International, Inc., Pittsburgh, PA 15224, USA

Received 21 August 1983

A theoretical analysis of the membrane current distribution is carried out for a typical three-compartment electrolyser in order to point out the effects of geometry on the design of mesh anodes. The factors considered here include the introduction of an insulated border, the perforation of the anode, the finite conductivity of the substrate, and the introduction of a bus bar connection between the anode and the current lead. It is recommended that no insulated border be introduced, since, while reducing the anode area and consequently its cost, it leads to a nonuniform membrane current distribution and hence decreases membrane efficiency. Also, titanium is found to be a suitable substrate for the anode in spite of its relatively low conductivity.

Nomenclature

a	Dummy variable in Equation 3
b	Border width
b^*	Effective border width
f	Fraction of open area in electrode
F_B	Parameter defined by Equation 4
F_p	Parameter defined by Equation 8
F_{be}	Parameter defined by Equation 15
I	Total cell current
i	Local current density on the membrane at a point
i_∞	Current density along the membrane far from the border
$\bar{i}_{loc}$	Average value of current density over a small portion of the membrane
$\bar{i}_{cell}$	Average value of current density over the whole membrane
$\bar{i}_\infty$	Average value of current density on membrane far from the border
i_{max}	Maximum value of current density on membrane
$\bar{i}_{loc,max}$	Maximum value of $\bar{i}_{loc}$ on membrane due to electrode and bus bar resistance effects
i_p	Maximum value of current density over a single electrode perforation
j	$(-1)^{1/2}$
l_p	Characteristic length of mesh
L	Dimension of anode in the direction of bus bar orientation
L'	Dimension of anode in the direction perpendicular to bus bar
L''	Width of bus bar
s	Interelectrode gap
s_1	Membrane to anode gap
R	Electrolyte and membrane resistance
x_b	Coordinate along length of bus bar
x_B	Coordinate in border effect analysis
x_e	Coordinate along electrode in the analysis of its resistance effect
x_p	Coordinate in perforation effect analysis
δ_b	Bus bar thickness
δ_e	Electrode thickness
ρ_b	Bus bar resistivity
ρ_e	Electrode resistivity
ρ_{em}	Resistivity of metal in electrode
ϕ_b	Potential at a point on the bus bar
ϕ_e	Potential at a point on the electrode
$\bar{\phi}_e$	Average potential over the electrode
ϕ_{max}	Potential at the current source
ϕ_{cath}	Potential at the equipotential cathode

0021–891X/84 $03.00 + .12

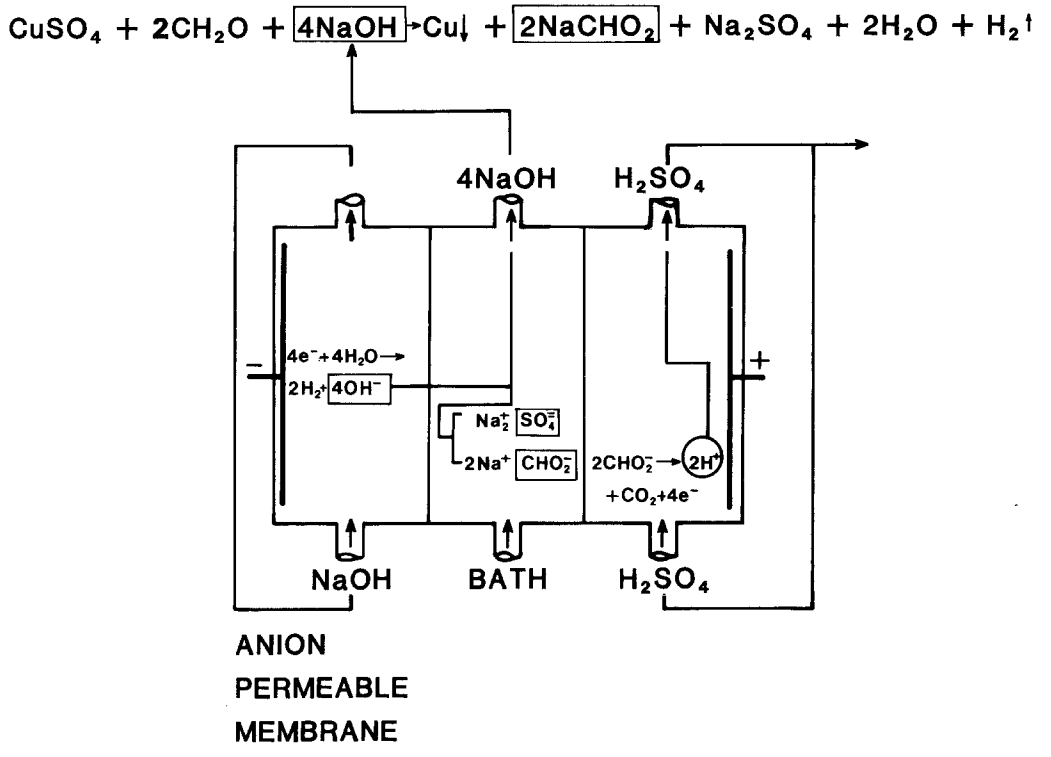

Fig. 1. The three-compartment membrane cell for regenerating electroless copper solutions as given by Horn [4].

1. Introduction

The membrane performance in an electrochemical cell is often dependent on the local current density. Examples of such processes include chlor-alkali membrane cells [1], batteries and fuel cells [2] and electrodialysis systems [3]. An example of an electrodialysis cell which utilizes two membranes is described by Horn [4]. This process is for regenerating caustic and removing reaction products in an electroless copper plating bath. A schematic of the process is shown in Fig. 1 and more details of the cell are depicted in Fig. 2. The cell is divided into three compartments. Caustic of 0.5 N aqueous solution flows through the cathode compartment, where hydroxide ion is produced at the cathode; the hydroxide ion passes through an anionic membrane to the centre compartment, thus replacing the caustic which was consumed in the electroless plating process. The impurity anions (sulphate and formate) are transported through a second anionic membrane to the anode compartment, in which water is injected and hydrogen ions are generated producing sulphuric acid and formic acid. Some formic acid is oxidized at the anode to CO_2 and water. The process is capital intensive to which the anode makes a significant contribution.

The problem is to minimize the cost of the anode, which must be coated with precious metal to provide a reactive area and, therefore, embodies much of the cost of the cell. There are two constraints on the design:

1. the electrode must be designed so as to minimize nonuniformities on the membranes. In particular, the anode will affect the membrane nearer to it, so this membrane will be of primary concern. A uniform membrane current distribution is necessary in order to maintain high membrane efficiency.
2. an adequate operating lifetime should be ensured for the coating on the electrode itself.

This paper considers the first of these design constraints. In particular the effect of the following design considerations on membrane current distribution will be examined.

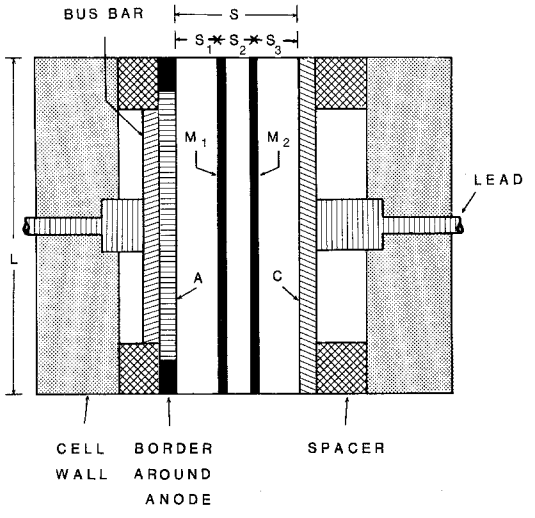

Fig. 2. Schematic view of three-compartment membrane cell.

1. *An insulated border on the anode.* One simple way of reducing the electrode area and cost is to introduce an insulated border around the anode. This, however, raises the effective current density and makes it nonuniform on the membrane.

2. *Electrode perforation.* To allow gas release and reduce electrode cost, perforations are included. This creates local current density variations on the membrane.

3. *Electrode resistance.* The flow of current through an electrode substrate of finite resistivity results in a voltage drop within the substrate and, consequently, leads to nonuniform current distribution.

4. *Bus bar resistance and placement.* The use of a properly sized and placed bus bar can aid in reducing substrate resistance effects and help create a more uniform current distribution. However, a bus bar does contribute another resistance in series to the system.

Each of these considerations will be treated separately. Finally, the net effect of all the considerations will be examined in terms of a practical example.

2. Background and approach

A considerable amount of work has already been done on the analysis of current distributions on the electrodes of an electrochemical reactor. Reviews of some of the current distribution problems which have been tackled in the literature have been provided by Newman [5] and Pickett [6]. More current work has been summarized in conference proceedings [7, 8]. Recently Lee and Selman [9] reported a study of the current distribution in a channel electrolyser with parallel planar electrodes. They followed the approach of Parrish and Newman [10] but included the effect of the membrane and substrate ohmic losses. The solution method was by orthoganol collocation similar to that reported by Caban and Chapman [11]. This study differs from but complements the studies of Lee and Selman [9] and others by placing the emphasis on the current distribution on the membrane.

In this study the effect of an anode border, and the effect of the anode mesh structure on the current distribution on a membrane separating the anode compartment from the cathode compartment is analysed. The approach is to solve the Laplace equation in the field between the two electrodes for the primary distribution:

$$\nabla^2\phi = 0 \tag{1}$$

The effect of the membrane on the potential field is neglected and the cathode is assumed to be very conductive and thus to be uniform and equipotential. Other assumptions and boundary conditions are introduced as the various effects are considered.

The solution of the Laplace equation for the primary current and potential distributions has been determined for many cell systems. Some examples are calculations of the effective resistance between two electrodes as reported by Kasper [12–14] for a variety of geometries and by Moulton [15] for the arbitrary placement of electrodes on the walls of a rectangular channel. Hine [16] calculated the current distribution on the front and back sides of two parallel planar electrodes within an insulating container where the electrodes do not contact the sides of the container. Newman [17] gives a review of the mathematical techniques of obtaining current distributions in electrochemical cells.

3. Analysis

3.1. *Cell structure and design factors considered*

The structure in Fig. 2 will now be examined in detail. The anode (A) is a titanium mesh, coated on the front side with platinum or other precious metal. An insulated border is included, since this represents a possible method of reducing the area and cost of the electrode. The resistivity of the anode is relatively high ($\rho_{Ti} = 7.2 \times 10^{-5}\ \Omega$ cm [18]) and this necessitates a heavy bus bar along the length of the anode. The cathode (C) is simply a stainless steel mesh. Two membranes (M_1, M_2) separate the cell into three compartments. Since this study is focused on the anode design, attention will be centred on the current distribution on M_1, located at a distance s_1 from the anode. Spacers are interspersed with fluid in the anode and cathode compartments to support the membranes. There is also a cavity behind each electrode to allow for the disengagement of evolved gas through the electrode meshes.

The structure described above leads to three sources of nonuniformity on the membrane M_1:

1. The insulated border, of width b, placed around the outside of the anode to reduce its area.
2. The perforation of the anode, necessary for the removal of gas bubbles.
3. The resistance of the bus bar and anode.

Each of these factors will now be considered in turn.

3.2. *Border effect*

The effect of the insulated border on the current distribution on M_1 will now be determined.

Fig. 3a depicts the pertinent dimensions for determination of the border effect. The overall dimensions of the electrode are L and L', and the border is taken to be of width b. Fig. 3b shows a two-dimensional approximate model of the system. If the cell is assumed homogeneous, and L and L' are large compared to b and s, then the primary normal current distribution along M_1 can be found by solving the Laplace equation using conformal mapping and standard transformations [19]. The result is the following expression

$$\frac{\bar{i}_{loc}}{\bar{i}_\infty} = \text{Real}\left\{\frac{\cosh\left[\pi(x_B/s + js_1/s)\right] - 1}{\cosh\left[\pi(x_B/s + js_1/s)\right] - \cosh\left[\pi b/s\right]}\right\}^{1/2} \tag{2}$$

where $\bar{i}_{loc}$ is the average current density over a region that is large compared to the perforations but small compared to the electrode, i_∞ is the current density along the membrane far from the border. Fig. 4 shows the distribution in graphical form for two cases. Note that if $s_1/s < 0.5$, then there is a maximum in the curve; this may be eliminated by designing the cell so that $s_1/s \geqslant 0.5$.

As expected, the current 'fringes' in the interelectrode gap so that the effective border width, b^*, is less than b. The effective border width is given by

$$b^* = \lim_{a\to\infty}\left[a - \frac{1}{\bar{i}_\infty}\int_0^a \bar{i}_{loc}\,dx_B\right] \tag{3}$$

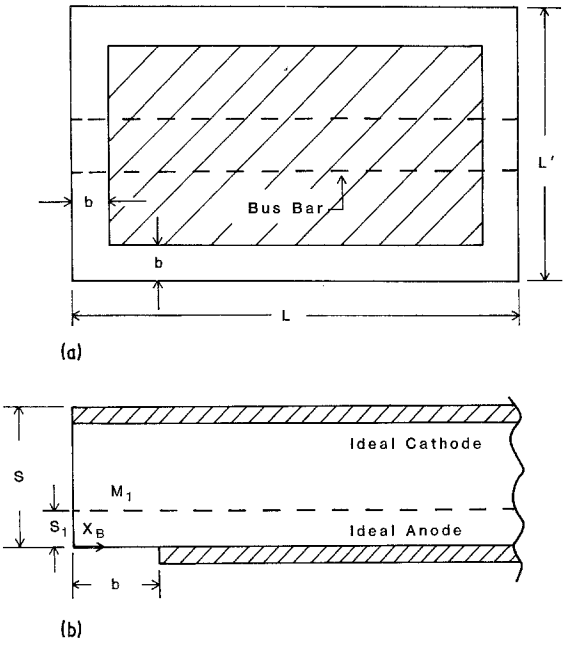

Fig. 3. Schematics of (a) electrode and (b) cell section, for border effect analysis.

With this effective border width the current density on M_1 at points far from the border may be written thus:

$$\frac{\bar{i}_\infty}{\bar{i}_{\text{cell}}} \equiv F_B = \frac{LL'}{(L-2b)(L'-2b)} = \frac{\text{total area}}{\text{total effective area}} \tag{4}$$

Equation 3, when combined with Equation 2, gives:

$$b^* = \frac{2s}{\pi} \ln [\cosh (\pi b/2s)] \tag{5}$$

Fig. 5 shows the relationship in dimensionless graphical form.

If b^* were considerably less than b, then it would be possible to introduce a significant border without adversely affecting the current distribution on the membrane simply by setting $(s_1/s) \geqslant 0.5$, since

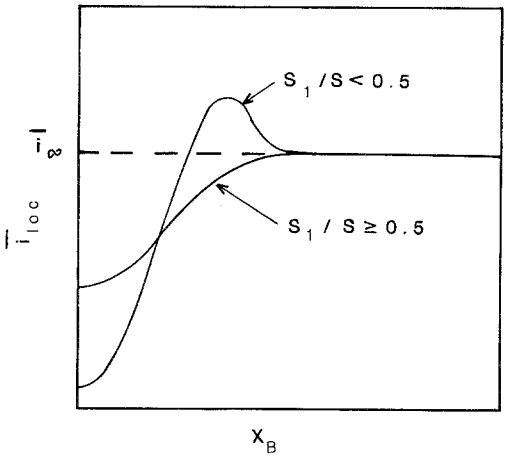

Fig. 4. Primary normal current distribution on M_1 in border effect analysis.

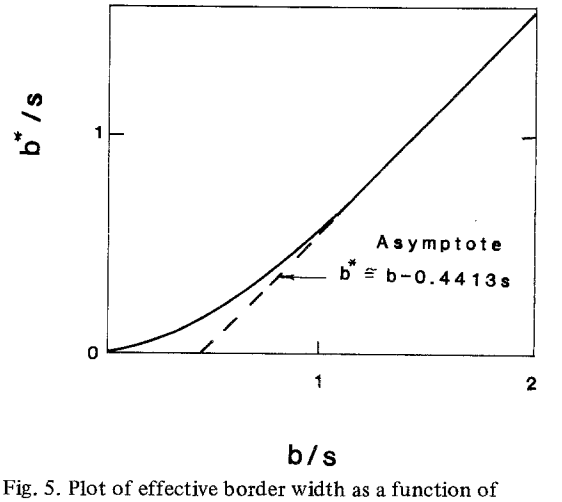

Fig. 5. Plot of effective border width as a function of actual border width.

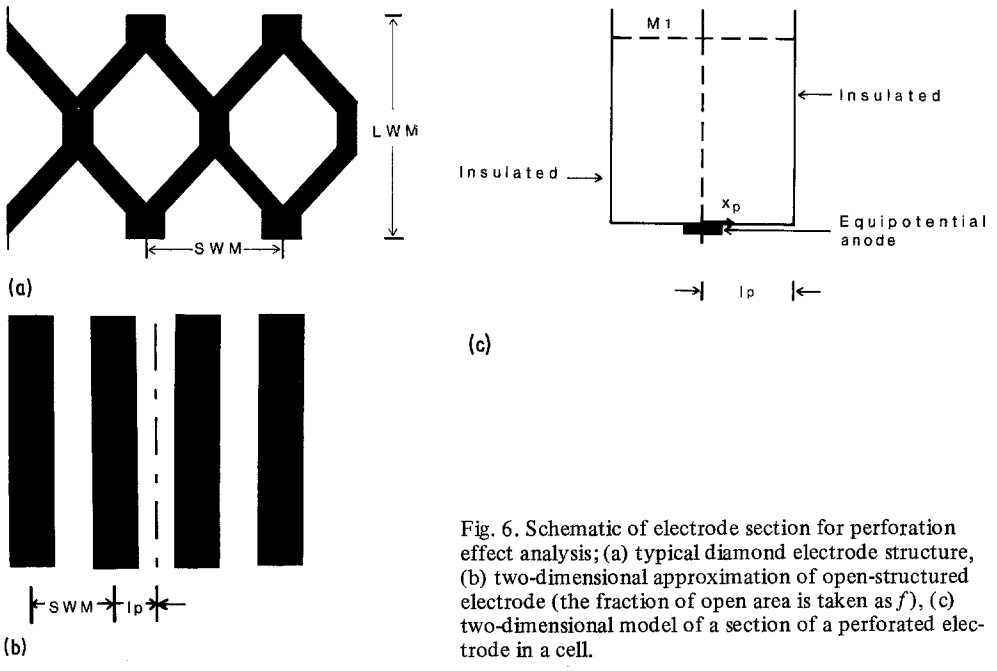

Fig. 6. Schematic of electrode section for perforation effect analysis; (a) typical diamond electrode structure, (b) two-dimensional approximation of open-structured electrode (the fraction of open area is taken as f), (c) two-dimensional model of a section of a perforated electrode in a cell.

then $\bar{i}_\infty/\bar{i}_{\text{cell}}$, given in Equation 4, represents the greatest factor by which the border alone raises the current density over any part of the membrane. Unfortunately, Fig. 5 shows that this is not the case; in fact $b - b^* \leqslant 0.4413s$, and since s is kept small to minimize ohmic potential drop and space requirements, it is apparent that even a small border may raise the current density considerably over much of the membrane while leaving the rest of the membrane essentially unused. This lowers the efficiency of the process, particularly when one considers other effects such as the dependency of membrane transport properties on local current density. Thus, as a preliminary conclusion, it is found that introducing a border is impractical.

3.3. *Perforation effect*

The second factor to be considered is the effect of electrode perforation on membrane current distribution.

Both the anode and cathode must be perforated to allow for gas release. Perforated electrodes, however, do not give a uniform current distribution over a membrane surface if the open areas relative to the closed areas are large and the membrane is placed too near the electrode.

Fig. 6a shows a typical diamond mesh structure. This may be approximated by the planar, periodic structure of Fig. 6b. The period is set equal to the Short Way of Mesh (SWM) dimension of the electrode. The fraction of the open area is defined as f. The geometry of Fig. 6c may be used to obtain a current distribution at the membrane, M_1. Proceeding in a fashion similar to the treatment of the border effect, the local primary current distribution, i, due to the perforation effect, on M_1, can be described by the following:

$$\frac{i}{\bar{i}_{\text{loc}}} = \text{Real}\left\{1 - \frac{\cos^2[\pi(1-f)/2]}{\cos^2[\pi(x_p/l_p + js_1/l_p)/2]}\right\}^{-1/2} \tag{6}$$

If s_1/l_p is about 1 or larger, this simplifies to

$$\frac{i}{\bar{i}_{\text{loc}}} \equiv 1 + \left\{\cos^2\left[\frac{\pi(1-f)}{2}\right]\right\}[2e^{-\pi s_1/l_p}\cos(\pi x_p/l_p)] \tag{7}$$

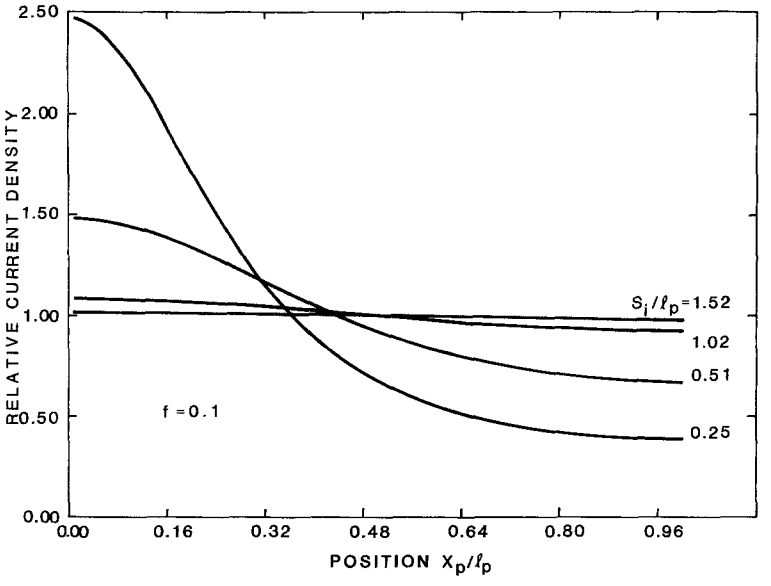

Fig. 7. Local current distribution of membrane due to perforation.

which is sinusoidal, as expected. Fig. 7 depicts a few typical cases of Equation 6 in graphical form. From Equation 6, the maximum in current density occurs at $x_p = 0$ so that

$$\frac{i_p}{\bar{i}_{loc}} \equiv F_p = \left\{1 - \frac{\cos^2[\pi(1-f)/2]}{\cosh^2[\pi s_1/2\ell_p]}\right\}^{-1/2} \tag{8}$$

3.4. *Electrode and bus bar resistance*

Up to this point, the major concern has been focused on the primary current distributions. In fact, the anode is not a perfect equipotential surface. There is some voltage drop across it, especially since the substrate (often titanium) has a relatively high resistivity. Lee and Selman [9] and Scott [20] have demonstrated the importance of this resistance. Hence, its effect on membrane current distribution must be examined.

Figs. 8a and b are close-up views of the bus bar and anode showing the direction of the current flow.

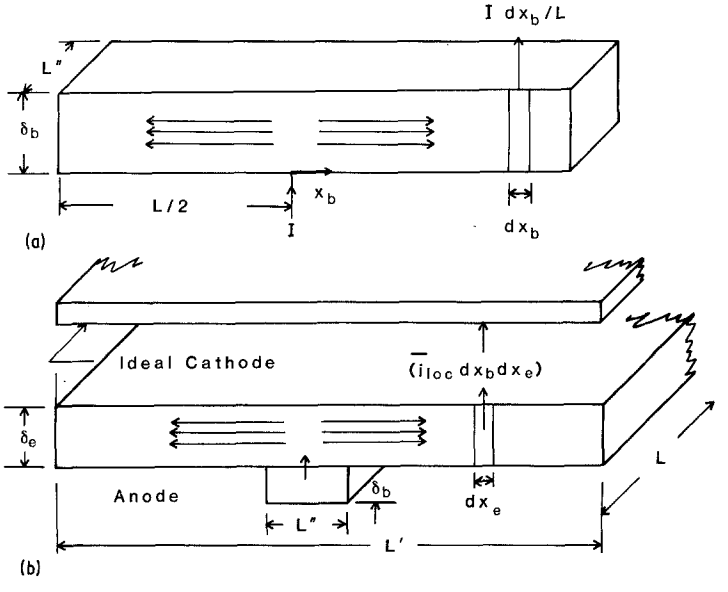

Fig. 8. Flow of current through the (a) bus bar and (b) the anode and interelectrode gap.

Since the cathode material is usually very conductive and less costly, it can be made so that it is equipotential, this assumption is incorporated into Fig. 8b.

Let it be assumed that the source of current is at a potential ϕ_{max} and that the bar uniformly distributes current over the length L of the electrode. Then, along the bar, a voltage balance gives:

$$\phi_b = \phi_{max} - \frac{I\rho_b|x_b|(L-|x_b|)}{2LL''\delta_b} \tag{9}$$

Over an element of width dx_b on the electrode, the bar then provides a source current Idx_b/L at potential ϕ_b. Then, assuming that the electrode distributes current approximately uniformly to the electrolyte, one obtains:

$$\phi_e = \phi_b - \frac{I\rho_e|x_e|(L'-|x_e|)}{2LL'\delta_e} \tag{10}$$

Equations 9 and 10 may be combined to give:

$$\phi_e = \phi_{max} - \frac{I}{2L}\left[\frac{\rho_b|x_b|(L-|x_b|)}{L''\delta_b} + \frac{\rho_e|x_e|(L'-|x_e|)}{L'\delta_e}\right] \tag{11}$$

But, the current flow in the electrolyte is essentially unidirectional (except for the perforation effect, considered separately) so that a voltage balance across the electrolyte gives

$$\frac{\bar{i}_{loc,max}}{\bar{i}_{cell}} = \frac{\phi_{max}-\phi_{cath}}{\bar{\phi}_e-\phi_{cath}} \tag{12}$$

where ϕ_{cath} is the cathode potential, which is assumed constant. The average electrode potential is found from Equation 10 to be:

$$\bar{\phi}_e = \phi_{max} - \frac{I}{12}\left(\frac{\rho_b L^2}{LL''\delta_b} + \frac{\rho_e L'^2}{LL'\delta_e}\right) \tag{13}$$

If the effective electrolyte and membrane resistance is R, then:

$$\bar{\phi}_e - \phi_{cath} = \bar{i}_{cell}LL'R = IR \tag{14}$$

Solving Equation 13 for ϕ_{max} and Equation 14 for ϕ_{cath}, and substituting into Equation 12 yields:

$$\frac{\bar{i}_{loc,max}}{\bar{i}_{cell}} = 1 + \frac{1}{12}\left[\frac{\rho_b L}{RL''\delta_b} + \frac{\rho_e L'}{RL\delta_e}\right] \equiv F_{be} \tag{15}$$

This development is valid when the groups $\rho_b L^2/4RLL''\delta_b$ and $\rho_e L'^2/4RLL'\delta_e$ are less than 0.6. Since the aim of the design is to minimize these dimensionless groups so as to minimize F_{be}, this is a reasonable assumption. Scott [20], Tobias and Wijsman [21], Vaaler [22], and Rousar *et al.* [23] have treated the resistance effect more rigorously in similar systems without membranes.

The electrode resistivity ρ_e is not a function of the metal alone. It is also affected by perforation, since the openings have no conductivity. Thus, if ρ_{em} is the resistivity of the electrode metal, then the following expression, which is essentially a two-dimensional Maxwell equation, may be used:

$$\frac{\rho_e}{\rho_{em}} = \frac{1+f}{1-f} \tag{16}$$

4. Application of theory and discussion

The application of the above equations to actual cells is now considered. Equation 8 gives a ratio of maximum current density to local average current density for a perforated electrode. The local average current density varies over the electrode, and its maximum, relative to the average current density over the effective electrode area, is given by Equation 14. Equation 4 provides the correction for the border,

Table 1. Values of parameters used in calculations summarized in Table 2

Case	*Cell dimensions*		*Bus bar dimensions*		*Electrode thickness*	*Mesh specifications*	
	L *(cm)*	L′ *(cm)*	L″ *(cm)*	δ_b *(cm)*	*dimensions* δ_e	*SWM*	f
a	65.723	37.783	2.54	0.0794	0.0794	0.508	0.50
b	37.783	65.723	2.54	0.159	0.159	0.508	0.76
c			3.81	0.0794		0.635	0.50
d			3.81	0.159		0.635	0.76
	$s_1 = 0.254$ cm				$b = 0$ ($F_B = 1$)		

Properties. $R = 0.008$ ohm, titanium bus and electrode, $\rho_{em} = 7.2 \cdot 10^{-5}$ Ω cm [18].

but this is impractical, as has already been shown. Thus, the ratio of maximum to average current density is given by:

$$\frac{i_{max}}{\bar{i}_{cell}} = \frac{\bar{i}_{loc,max}}{\bar{i}_{cell}} + \frac{\bar{i}_{loc,max}}{\bar{i}_{cell}}\left(\frac{i_p}{\bar{i}_{loc}} - 1\right) = F_p F_{be} \tag{17}$$

Once i_{max} is known, one can determine whether the nonuniformities in the current distribution affect the efficiency, since it is in regions of high current density that inefficiencies occur. Table 1 gives some cell specifications which are used to exemplify the use of Equations 8 and 15, including Equation 16, which is needed for the use of Equation 15.

Cases a and b for the 'Cell dimensions' correspond to placing a bus bar along the length and width of the electrode, respectively. Cases a–d for the 'Bus bar dimensions' are concerned with examining the effects of the bus bar width and thickness. Cases a and b of 'Electrode dimensions' are included to investigate the effect of electrode thickness. The mesh size and perforation area are varied in the 'Mesh specifications'. Thus 64 cases in all are tested. The results are summarized in Table 2.

The bus bar resistance is seen to be important, so that in most of the cases studied the bus bar placed across the width is preferred. However, there are cases where the electrode resistance may be sufficiently large so that the alternative configuration, which has more bus bar resistance but less electrode resistance, may be preferable. This is particularly true for thinner electrodes. Generally, $F_{be} > F_p$, so that the local nonuniformities due to perforation are not as important as those due to the electrode and bus bar

Table 2. Calculated current distribution parameters from Equations 8 and 15 with parameter values given in Table 1

Cell dimensions	*Bus bar dimensions*	*Electrode dimensions*	*Mesh specifications*	F_p	F_{be}	i_{max}/i
a	a	a	a	1.042	1.261	1.314
a	a	a	b	1.077	1.284	1.383
a	a	a	c	1.077	1.261	1.358
a	a	a	d	1.147	1.284	1.473
a	a	b	a	1.042	1.245	1.297
a	a	b	b	1.077	1.264	1.362
a	a	b	c	1.077	1.245	1.341
a	a	b	d	1.147	1.264	1.450
a	b	a	a	1.042	1.138	1.186
a	b	a	b	1.077	1.161	1.250
a	b	a	c	1.077	1.138	1.227
a	b	a	d	1.147	1.161	1.332
a	b	b	a	1.042	1.130	1.177*
a	b	b	b	1.077	1.142	1.220
a	b	b	c	1.077	1.130	1.217
a	b	b	d	1.147	1.142	1.310

Table 2. (Continued)

Cell dimensions	*Bus bar dimensions*	*Electrode dimensions*	*Mesh specifications*	$[F_p]$	$[F_{be}]$	$[i_{max}/i]$
a	c	a	a	1.042	1.179	1.229
a	c	a	b	1.077	1.203	1.295
a	c	a	c	1.077	1.179	1.270
a	c	a	d	1.147	1.203	1.380
a	c	a	a	1.042	1.171	1.220
a	c	a	b	1.077	1.183	1.274
a	c	a	c	1.077	1.171	1.261
a	c	a	d	1.147	1.183	1.357
a	d	a	a	1.042	1.098	1.144*
a	d	a	b	1.077	1.121	1.208
a	d	a	c	1.077	1.098	1.183*
a	d	a	d	1.147	1.121	1.286
a	d	b	a	1.042	1.090	1.136*
a	d	b	b	1.077	1.102	1.187*
a	d	b	c	1.077	1.090	1.174*
a	d	b	d	1.147	1.102	1.264
b	a	a	a	1.042	1.190	1.240
b	a	a	b	1.077	1.261	1.358
b	a	a	c	1.077	1.190	1.282
b	a	a	d	1.147	1.261	1.446
b	a	b	a	1.042	1.165	1.214
b	a	b	b	1.077	1.201	1.293
b	a	b	c	1.077	1.165	1.255
b	a	b	d	1.147	1.201	1.378
b	b	a	a	1.042	1.120	1.167*
b	b	a	b	1.077	1.191	1.282
b	b	a	c	1.077	1.120	1.206
b	b	a	d	1.147	1.191	1.366
b	b	b	a	1.042	1.095	1.141*
b	b	b	b	1.077	1.131	1.218
b	b	b	c	1.077	1.095	1.179*
b	b	b	d	1.147	1.131	1.298
b	c	a	a	1.042	1.143	1.191*
b	c	a	b	1.077	1.214	1.308
b	c	a	c	1.077	1.143	1.231
b	c	a	d	1.147	1.214	1.392
b	c	b	a	1.042	1.118	1.165*
b	c	b	b	1.077	1.154	1.243
b	c	b	c	1.077	1.118	1.205
b	c	b	d	1.147	1.154	1.324
b	d	a	a	1.042	1.096	1.142*
b	d	a	b	1.077	1.167	1.257
b	d	a	c	1.077	1.096	1.180*
b	d	a	d	1.147	1.167	1.339
b	d	b	a	1.042	1.072	1.117*
b	d	b	b	1.077	1.107	1.192*
b	d	b	c	1.077	1.072	1.154*
b	d	b	d	1.147	1.107	1.270*

* Less than 20% maximum positive deviation.

resistance. However, the size of the mesh does significantly influence F_p; even a 25% increase in the SWM approximately doubles the nonuniformity. Hence, the mesh should be kept small, but not to the point where gas release is hindered. In some situations high perforation can be used if gas release is improved significantly and electrode life remains acceptable; however, the benefits are limited and are at the expense of a more nonuniform membrane current distribution, as both F_p and F_{be} depend on the perforation through the parameter f.

Finally, since most electrode reactions in electrodialysis systems are water splitters, the effect of gas bubbles should be mentioned. Gas bubbles released from the electrode reactions accumulate at the top of the cell. As a result, the electrolyte resistance increases from the bottom to the top of the cell, thus causing a nonuniform current distribution with the higher current density at the bottom. An estimation of the magnitude of this effect requires additional information such as electrolyte velocities. Induced pumping will decrease the nonuniformity of current distribution [24]. Another approach would be to use a vertical bus bar which does not extend to the bottom of the anode. This will result in additional substrate resistance at the bottom of the anode and thus offset some of the effects of the increased resistance at the top of the cell. One disadvantage with this approach is the additional cell voltage.

5. Summary

In this paper several simple mathematical expressions relating to some anode design factors have been presented which allows one to estimate the nonuniformity of membrane current density. By utilizing these expressions several conclusions have been made regarding the design of a titanium mesh anode for a membrane cell.

1. Introduction of an insulated border around the anode area, while reducing the anode area and its costs, reduces the effective membrane area of current passage by an almost equal amount, so that such a border is impractical for capital economies.

2. Titanium, even with its relatively low conductivity, is a reasonable choice for a substrate. Substrate conductivity is not a critical factor. A bus bar, however, should be used to improve electrode conductance.

3. Care must be taken to ensure that the bus bar has a reasonably good conductance.

4. Perforations should not be made too large, since perforation size strongly affects the size of local current density variation on the membrane.

Acknowledgement

The authors wish to acknowledge the computer programming assistance provided by T. Borgen. Also, the financial assistance from Electrochem International is greatly appreciated.

References

[1] D. L. Caldwell, in 'Comprehensive Treatise of Electrochemistry', Vol. 2 (edited by J. O'M. Bockris, B. E. Conway, E. Yeager and R. E. White) Plenum Press, New York (1981) Ch. 2.
[2] R. Yeo, in 'The Perfluorinated Ionomer Membranes' (edited by A. Eisenberg, and H. Yeager) ACS Symposium Series No. 180, American Chemical Society, Washington, D.C. (1982).
[3] G. S. Solt, in 'Industrial Electrochemical Processes' (edited by A. T. Kuhn) Elsevier Publishing, New York (1971) Ch. 12.
[4] R. E. Horn, *Plat. Surf. Finish.* 68 (1981) p. 50.
[5] J. S. Newman, 'Electrochemical Systems', Prentice-Hall, Englewood Cliffs, New Jersey (1973).
[6] D. J. Pickett, 'Electrochemical Reactor Design', Elsevier, Amsterdam (1979).
[7] R. Alkire and T. Beck (Eds.), 'Tutorial Lectures in Electrochemical Engineering and Technology', AIChE Symposium Series, Vol. 77, No. 204, AIChE, New York (1981).
[8] M. Krumpelt, E. Y. Weissman and R. C. Alkire, (Eds.) 'Electro-organic Synthesis Technology', AIChE Symposium Series, Vol. 75, No. 185, AIChE, New York (1979).

[9] J. Lee and J. R. Selman, *J. Electrochemical Soc.* **129** (1982) 1670.
[10] W. R. Parrish and J. Newman, *ibid.* **117** (1970) 43.
[11] R. Caban and T. W. Chapman, *ibid.* **123** (1976) 1036.
[12] C. Kasper, *Trans. Electrochem. Soc.* 77 (1940) 353.
[13] *Idem, ibid.* **78** (1940) 131.
[14] *Idem, ibid.* **82** (1942) 153.
[15] H. F. Moulton, *Proc. London Math. Soc.* (*Sec. 2*) **3** (1905) 104.
[16] F. Hine, S. Yoshizawa and S. Okada, *J. Electrochem. Soc.* **103** (1956) 186.
[17] J. Newman, in 'Electroanalytical Chemistry', Vol. 8 (edited by A. J. Bard) Marcel Dekker, New York (1972).
[18] R. O. Loutfy and R. L. Leroy, *J. Appl. Electrochem.* **8** (1978) 549.
[19] M. R. Spiegel, 'Complex Variables', Schaum's Outline Series, McGraw-Hill, New York (1964).
[20] K. Scott, *J. Appl. Electrochem.* **13** (1983) 209.
[21] C. W. Tobias and R. Wijsman, *J. Electrochem. Soc.* **100** (1953) 459.
[22] L. E. Vaaler, *ibid.* 9 (1979) 21.
[23] I. Rousar, V. Cezner, J. Nejapsova, M. M. Jacksic, M. Spasojevic and B. Z. Nikolic, *ibid.* 7 (1977) 427.
[24] F. Hine and K. Murakami, *J. Electrochem. Soc.* **128** (1981) 128.